Characteristics of Welding Fumes

Johansson, Gerd; Malmqvist, Klas; Bohgard, Mats; Akselsson, Roland

1981

Dokumentutgivare
Lunds Universitet
Handläggare
Klas Malmqvist
Författare

Dokumentnamn
rapport
Utgivningsdatum
21/8 1981

Dokumentbeteckning
LUTFD2/TFKF-3030/(1981
Ärendebeteckning

Gerd I Johansson, Klas G Malmqvist, Mats Bohgard och K Roland Akselsson
Inst för kärnfysik, LTH, Sölvegatan 14, 223 62 Lund

Dokumenttitel och undertitel

Characteristics of welding fumes

Referat (sammandrag)

The aerosols from 13 common electric arc welding processes have been characterized regarding total mass emission, particle size distribution, elemental composition and, when applicable, the oxidation state of chromium. The characterizations have been performed systematically for different combinations of welding current and welding voltage.

Referat skrivet av
Författarna
Förslag till ytterligare nyckelord

Klassifikationssystem och -klass(er)

Indextermer (ange källa)

Omfång
32
Övriga bibliografiska uppgifter
Språk
Eng
Sekretessuppgifter
ISSN
ISBN
Dokumentet kan erhållas från
Mottagarens uppgifter
se författarnas adress ovan
Pris
gratis

LUTFD2/TFKF-3030/(1981)

CHARACTERISTICS OF WELDING FUMES

Gerd I. Johansson,[1,2] Klas G. Malmqvist,[1] Mats Bohgard[1] and K. Roland Akselsson,[1,2]

[1] Department of Nuclear Physics, Lund Institute of Technology,
Sölvegatan 14, S-223 62 LUND, SWEDEN.

[2] Department of Environmental Health, University of Lund,
Sölvegatan 21, S-223 62 LUND, SWEDEN.

ABSTRACT

The aerosols from 13 common electric arc welding processes have been characterized regarding total mass emission, particle size distribution, elemental composition and, when applicable, the oxidation state of chromium. The characterizations have been performed systematically for different combinations of welding current and welding voltage.

INTRODUCTION

In the work environment electric arc welding is a common process producing complex and abundant fumes. Since the distribution in size and elemental composition of the produced particles also vary within wide limits for different modes of operation, the finding of dose-response relations, the design of effective monitoring programmes and the choice of strategies for elimination techniques constitute a challenging task for industrial hygienists, epidemiologists, toxicologists, etc.. A fundamental prerequisite for the successful tackling of these central tasks is a thorough knowledge of the size distribution and composition of the welding aerosol particles. Although not dealt with explicitly in this work, in this connection other environmental factors, e.g. gaseous emissions, electromagnetic radiations and ergonomic aspects are of the outmost concern.

In a recent book, Moreton and Falla[1] have summarized existing information in the field of analysis and sampling of welding fumes while in a volume from the American Welding Society[2] the results of a major study of fumes and gases in the

the welding environment are reported. It is well known from other studies of welding aerosols that variations in current and voltage can influence the characteristics of the welding fumes produced[3,4,5].

To verify and extend existing information on welding aerosols, a comprehensive investigation of the total mass emission, particle size distribution, elemental composition and, when applicable, the oxidation state of chromium has been performed for 13 different welding methods (Table 1). The methods were chosen in cooperation with representatives of manufacturers and other experts on welding techniques and cover the three main types of welding: Shielded Metal Arc Welding (SMAW), Gas Metal Arc Welding (GMAW) and Gas Tungsten Arc Welding (GTAW). Most methods have been chosen from a Swedish firm manufacturing welding material, ESAB, which has an extensive export to the world market. In Table 1 the corresponding AWS classifications are, when possible, given.

Electrode		Type	Coating	AWS[a]-class.	Diam.(mm)	Gas
1	OK 38.65	SMAW	iron powder, low hydr. zirconium added	E 7028	3.25	-
2	OK 38.85	SMAW	iron powder, low hydr.- rutile	E 7028	5	-
3	OK 38.95	SMAW	iron powder, low hydr. zirconium added	E 7028	4	-
4	OK 48.00	SMAW	iron powder, low hydr.	E 7018	2,3.25,4	-
5	OK 61.41	SMAW[b]	rutile	E 308 L-15	3.25	-
6	OK 63.35	SMAW[b]	low hydrogen	E 316-15	2.5,3.25,4,5	-
7	OK 69.21	SMAW[b]	low hydrogen-rutile	-	3.25,4,5	-
8	OK 12.51	GMAW	-	E 70 S-6	1.2	CO_2
9	OK 16.32	GMAW[b]	-	ER 316 I Si	1.2	Ar
10	OK 16.32	GMAW[b]	-	ER 316 I Si	1.2	Ar/CO_2
11	OK 18.01	GMAW[c]	-	ER 1260	1.2	Ar
12	OK 18.13	GMAW[c]	-	ER 5154	1.2	Ar
13	Tungsten Th added	GTAW[b]	-	-	-	Ar

a) AWS-class. = American Welding Society classification.

b) welding on stainless steel; c) welding on aluminium.

Table 1. A list of the welding methods included in this study. The numbers are used for identification in the various figures.

Since size distributions and elemental compositions have been investigated for several sets of current and voltage for each of the 13 methods of welding studied, an extensive database has been created. In this paper the results are summarized. A complete listing of the results can be obtained from the authors[6].

MATERIAL AND METHODS

SAMPLING EQUIPMENT

Figure 1 shows the design of the sampling arrangement. The welding takes place beneath an aluminium hood. Two fans (ESAB, OFA, 13 kPa at 60 m^3/h) connected in series pull air through a glass fibre filter (Millipore AP, 2529325, diam: 293 mm) on top of a pipe connected to the hood, in which the welding fume is collected. This equipment allows reproducible and representative sampling of fume from manual and automatic welding processes. The low velocity of the air around the welding point (<0.15 m/s) assures that the sampling procedure has no significant impact on the welding process and aerosol formation.

The total mass of welding aerosol is determined by gravimetric analysis of the glass fibre filters. These are insensitive to relative humidity and static electricity and hence repeated weighing over periods of several weeks give variations well below 0.1 % of the filter weight. For the collections in this study, the uncertainty in the total mass determinations is, in all cases, below 5%.

During the welding of a rod the filter will gradually clog and the pressure drop over the filter increase. The air flow then decreases and limits the amount of fume which can be collected on one filter. Tests have demonstrated the sampling efficiency to be above 95% for the collection of 1000 mg of welding fumes (fig. 2), which is quite sufficient for the sampling situations in the present study.

Due to diffusion, minor losses of small particles to the walls of the sampling equipment occured. After a large number of collections ($\approx$100) the pipe and hood were washed with distilled water and the water filtered. The filters and filtrates were analysed for iron (PIXE analysis). A comparison between the mass of airborne iron produced and the mass deposited on the walls indicates that losses from the wall are less than one per cent of the total mass of fume produced. In this determination, large globular metal spatter has not been considered.

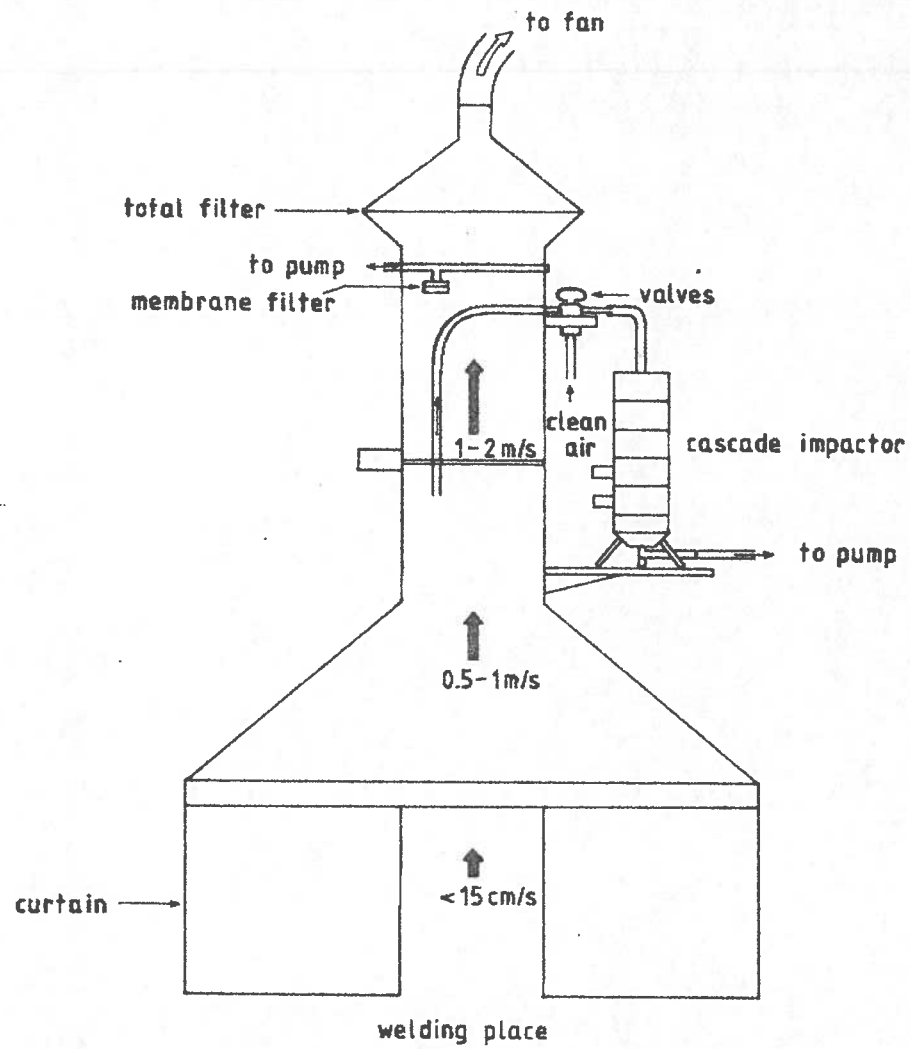

Figure 1. Sampling equipments for the characterization of welding aerosols. The arrows indicate the air velocity in different parts of the system.

The glass fibre filters are not well suited for chemical analysis since they contain high concentrations of impurities. Hence membrane filters made of mixed esters of cellulose (Millipore HAWP, diam.: 37 mm, pore diam.: 0.45 µm) have been used for determining the elemental composition of the aerosol. These filters contain insignificant concentrations of the elements of interest. A small portion of the total aerosol (<0.5%) is collected on the membrane filter for subsequent elemental analysis. To check for possible variations due to the filter orientation, three filters were placed in different positions inside the pipe facing the air stream. While welding, sampling was performed simultaneously with all three filters and the relative elemental composition was determined for each of them. The compositions of the three samples agreed well within 5%. Since the filter efficiency is approximately 100% for all particle sizes[7], the samples collected should be representative of the welding aerosol. However, due to the difference between the face velocity through the filter and the velocity in the tube, too many large particles will be collected from the aerosol. According to formulae given by Davies [8], the oversampling of particles with an aerodynamic

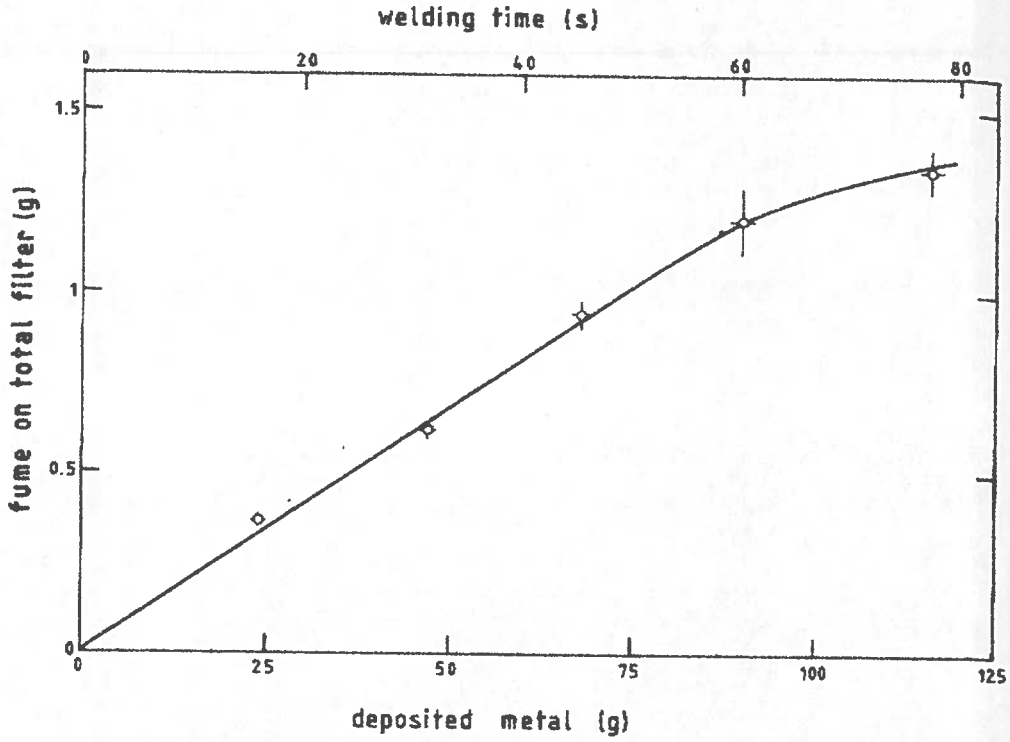

Figure 2. Performance of total fume sampling. Welding was performed with coated electrodes (OK 48.00) with a core diameter of 6 mm and a welding current of 300 A DC, reversed polarity. The error bars show one standard error of the mean.

diameter of less than 5 µm will be less than 10% and in previous studies[3,9] it has been shown that welding aerosols contain very few large particles (more than 95% of the mass represents particles with aerodynamic diameters less than 1 µm).

Since the membrane filter is used only for determining chemical composition, oversampling of certain fractions of particle sizes will only be important if different particle sizes have different compositions.

To determine the particle size distribution, a probe was inserted into the pipe facing the air stream to collect a small sample of the welding aerosol into a Battelle-type cascade impactor[10] placed outside the pipe wall. The nominal air-flow of this single orifice impactor was 1 litre/minute. The diameter of the probe was only 4 mm and to secure representative sampling, the sampling probe was allowed to move in a spiral back and forth over the entire cross section of the pipe. Several spirals were completed within a sampling period (30-60 seconds).

Since very dense aerosols are produced during welding and since the particle sizes which deposit on the two last stages in the impactor are predominant, the welding aerosol was diluted (1:10) by clean air (air drawn from outside the

building) before entering the impactor. Consequently the air velocity in the sampling tube from the probe will be low and diffusion losses of small particles will occur as will, sedimentation losses of large particles in the horizontal part of the tubing. These losses have been calculated[11] and are shown in fig.3. Since Reynolds number (Re) was about 50, i.e. well below the limit for turbulent flow (Re $\approx$2300), the losses have been calculated assuming laminar flow with no turbulent mixing. Although by restricting sampling to an interval of from about 0.01 to 3 µm these losses represent limiting factors, as was mentioned above, these particle sizes constitute more than 95% of the mass of the welding aerosols.

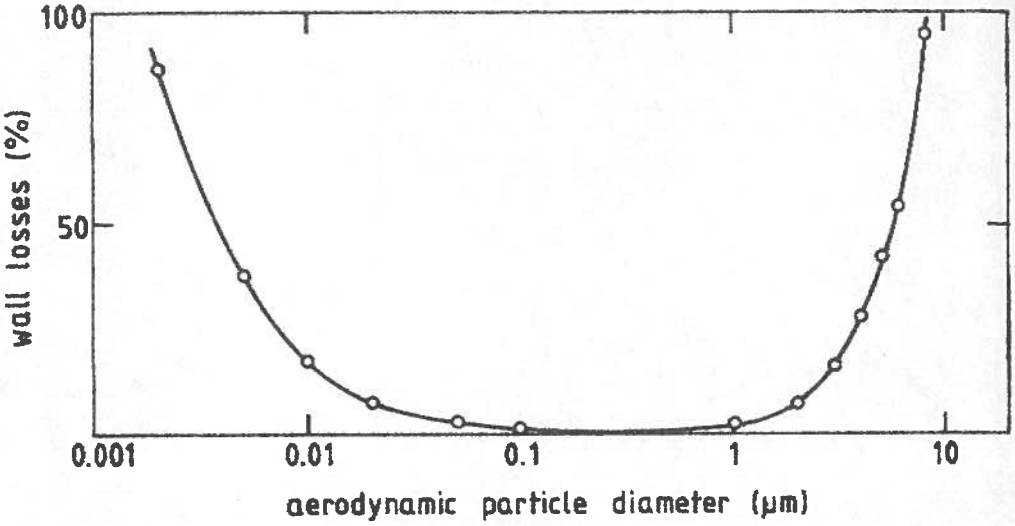

Figure 3. Calculated wall losses in the impactor tubing plotted versus particle diameter[11].

Similarly to the membrane filter the impactor probe samples subisokinetically. However, the oversampling (which occurs for particles with aerodynamic diameters larger than 5 µm), is insignificant since because of sedimentation any such particle, will not be able to penetrate the impactor tubing (see fig 3). Although the aerosol was diluted, for reasonable sampling times, some risks of overloading will still remain. Since even a slight overloading of the collection plates can severely alter the collection characteristics of a stage, further improvements have been carried out. By rotating the impaction plates off-axis during sampling, the particles are made to deposit over a larger area (30-60 times larger). This results in a significant improvement in collection performance and also facilitates accurate PIXE-analysis. Further details of this impactor modification are given in ref. 12.

ANALYTICAL METHODS

A brief description of the analytical procedures will be given here, but for a more detailed discussion see refs.[12,13,14,15].

The elemental composition of the welding aerosol samples collected has been determined mainly with the multielemental analytical method Particle Induced X-Ray Emission analysis, PIXE[12]. We have used protons (with an energy of 2.55 MeV) from an electrostatic accelerator to irradiate a sample (normal irradiation time 1-5 min). Vacancies are created in the inner shells of the atoms in the sample. When these vacancies are refilled, X-rays with energies characteristic of the atom from which they originate are emitted. Measuring these X-rays with a semiconductor detector (Si(Li), sensitive area = 10 mm^2, FWHM = 160 eV at 5.9 keV) in combination with suitable electronics will yield simultaneous quantitative results for all elements heavier than about phosphorous, with detection limits of the order of nanograms (1 ng = 10^{-9} g). In fig.4 is shown an example of a typical X-ray spectrum from the irradiation of a sample of welding fumes.

For the analysis of one important light element, fluorine, we detect simultaneously the gamma rays produced in the nuclear reaction $^{19}F(p,\alpha\gamma)^{16}O$ using a large volume sodium iodide crystal (detection limit 100 ng)[16]. Thin fluoride targets of known thicknesses are used as standards for quantitative analysis.

Since in this investigation, more than 3000 multielemental analyses had to be performed, access to the PIXE method with nuclear complementary techniques was a necessary condition for its realization. However, only the elemental composition is determined by the PIXE-method. Since in the case of chromium the oxidation state and probably also the solubility[17] are of major importance in evaluating health hazards, a special analytical procedure[15] was developed to quantify the masses of soluble and less soluble Cr(III) and Cr(VI). This procedure includes PIXE-analysis and complementary techniques such as Electron Spectroscopy for Chemical Analysis, ESCA[18], a spectrophotometric method, DPC[19] and transmission electron microscopy (TEM).

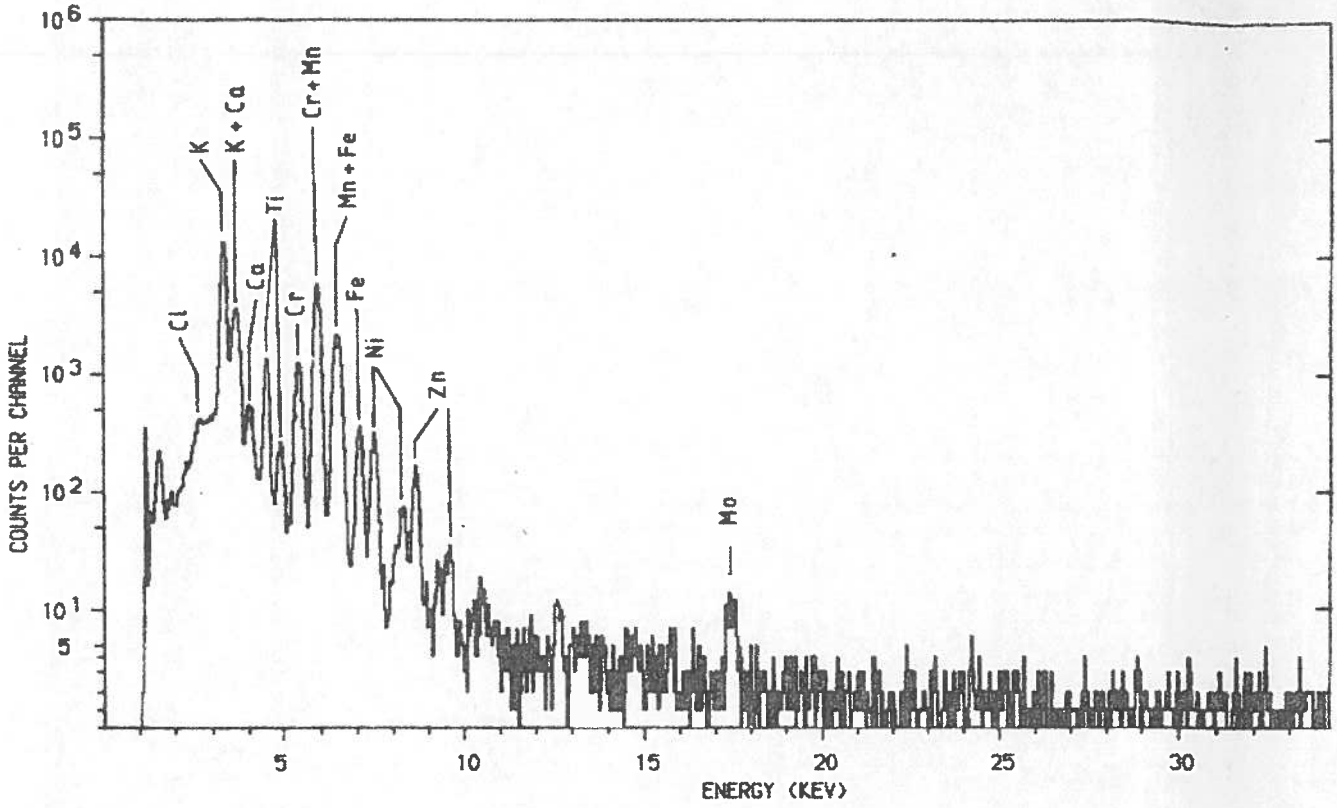

Figure 4. X-ray spectrum from the PIXE analysis of a welding fume sample (OK 69.21, I=140 A, U= 22 V) collected during stainless steel welding.

EXPERIMENTAL PROCEDURE

ANALYTICAL PROCEDURES

To determine the total masses of aerosols the pre-weighed glass fibre filters were re-weighed as soon as possible after collection. They were compared with pre-weighed blank filters to correct for possible systematic changes in filter weight. After weighing, a piece (3x3 cm^2) was punched from the filter and then transferred to a sample holder (a 5x5 cm^2 slide frame). The samples were analysed by PIXE for about 60 seconds to determine the iron content per unit area of the filter. From this the total mass of iron on the filter can be determined and by comparison with the total mass of aerosol, as determined by weighing, the relative iron content can be calculated. Except in the case aluminium welds, the iron concentration was then used as a reference for determining the elemental composition on the membrane filters.

By scanning the filter area with a proton beam, the homogeneity of the aerosol deposit on the filter surface has been determined to be better than 3%. Since sample thicknesses may sometimes exceed 1 mg/cm^2 , corrections for proton slowing-down and X-ray attenuation in the sample have been made. Taking this into account, the accuracy of the iron determination is typically 5%.

The membrane filters were weighed before and after sampling (using a Sartorius microbalance with a stated standard deviation of 1 µg). These filters were very sensitive to changes in relative humidity and to electrostatic build-up, although blank reference filters were used to correct for systematic weight changes due to the absorption of water and an α-emitting radioactive source and a piezo-electric decharger to reduce the effects of static electricity. Consequently, the gravimetric analyses were not sufficiently reliable for total aerosol mass determinations (the accuracy was in the interval from 10 to 30 %). The results were, however, used to double check the glass fibre filter determinations. After weighing, the filter was cut into two pieces one of which is glued to an aluminium frame which was mounted in a standard slide mount for PIXE analysis. The other half of the filter was stored in a Petri tray as a reserve sample. The sample was irradiated for 100 to 300 seconds with a proton current in the range from 5 to 50 nA using a proton beam area of 0.5 cm^2. The masses of all elements heavier than sulphur were determined and during the proton irradiation the 6 to 7 MeV gamma-rays from the $^{19}F(p,\alpha\gamma)^{16}O$ reaction were detected with a 5x4" NaI-crystal and counted for determining the fluorine content. While only 0.5 cm^2 of the total filter area was analysed during PIXE analysis, according to PIXE-measurements the aerosol deposit on the membrane filter was homogeneous within 2%, and hence the results were representative for the entire sample.

For stainless steel welding aerosols the chromium oxidation state was determined separately. Two parallel membrane filters collect aerosol in the pipe of the welding aerosol sampling set-up, giving mass differences between the two samples of less than 5%. A sample thickness from 0.05 to 0.1 mg/cm^2 is optimal for the analytical methods applied. One of the filters was washed with de-ionized water buffered with a solution of NH_4NO_3/NH_4OH to pH 7.4. One half of each filter, unwashed and washed respectively, was analysed with PIXE to determine the total and the less soluble chromium. The other halves of the filters were analysed with ESCA[18] which determines the oxidation state of the chromium in a 2 nm thick surface layer of the particles. To evaluate if the ESCA results were representative, another pair of parallel samples was taken and the individual welding aerosol particles were studied by transmission electron microscopy. The buffer solution containing the chromium which has been leached out was analysed with spectrophotometry using the DPC-reagent (diphenylcarbazide)[19].

In the cascade impactor for particle size determinations glass plates (Casella, diam: 25 mm) were used. Prior to use, these were cleaned and dipped into a

solution of polystyrene in toluene, which was then drained through a valve, slowly and at a constant speed. After drying a 30 $\mu g/cm^2$ thick polystyrene layer covered the plates. The plates were then placed 3 cm above a bath of melted hot paraffin (180 ^{o}C) and the paraffin vapour allowed to condense on the plates for 15 min, forming a "sticky" layer to reduce "bounce-off" of particles[20]. The glass plates were placed in the cascade impactor with the last four stages having 50 % cut-off diameters of 2, 1, 0.5 and 0.25 µm, respectively, followed by an after-filter (Nuclepore, diam.: 25 mm, pore diam.: 0.4 µm) to collect the smallest particles. After sampling, the plates were slowly put into de-ionized water and the polystyrene coatings with the aerosol samples floated off on to the surface of the water whence they were transferred to our standard aluminium frames. The latter were then mounted in the slide frames for subsequent proton irradiation for about 100-200 seconds, using a beam current of 50 to 150 nA and a 0.5 cm^2 beam area, sufficient to cover the samples completely. For the after-filter, the beam area was 0.13 cm^2 with a proton current of 30 to 50 nA and the analysis times from 200 to 300 seconds. Fluorine in the impactor samples was determined using the $^{19}F(p,\alpha\gamma)^{16}O$ reaction.

SAMPLING PROCEDURES

In Table 1 the different welding situations studied are summarized. The welding current was varied within the intervals recommended for each method and dimension by the manufacturer. The welding voltage was varied significantly outside "proper" welding conditions in order to show any possible systematic dependence of fume production on welding voltage.

Three to five collections were made for each set of welding parameters. The results are given as averages of the numbers of measurements made and the error limits given are one standard error of the mean. For some methods, e.g. GMAW on aluminium, only very restricted parameter intervals can be used for welding. The alternating current mode is recommended only for a few SMAW-methods and hence the influence of current mode on the welding aerosols has been studied for these methods only.

For the direct current SMAW-methods, an ESAB 400 welding generator is used in accordance with the instructions by the welding electrode manufacturer, i.e. reversed polarity (electrode positive). The welding is performed manually by a skilled welder exerting himself to maintain constant welding conditions.

Normally, the fumes from only one electrode are collected on one glass fibre filter but, to reduce weighing errors, for a few methods with very low fume emission several electrodes were welded. Current and voltage were recorded on a two-channel chart recorder. Voltage was measured between the electrode and the work piece and the current by a precision resistor in series with the welding generator. When AC-welding is carried out, a high current transformer was used.

For the GMAW-methods, an ESAB LBA 550 welding generator was used with the welding gun mounted in a fixed position perpendicular to the workpiece. The latter was clamped to an aluminium wagon running on rails with a very constant but variable speed to simulate the normal movement during welding. This automatic welding arrangement is necessary for the semi-automatic methods studied, since it is difficult to maintain constant conditions manually. Current and voltage were recorded in the same way as for the SMAW-methods. The wire feeding speed in GMAW-welding is adjustable and the setting was noted for each welding situation. They were calibrated by feeding the wire without welding for a certain time and measuring the amount of wire fed. The protective gas flow was monitored by a rotameter.

For GTAW-welding, a Miller DC welding generator is used. Due to the low emission rates from GTAW-processes, very long welding and collection times (30-40 min) were used.

The fans which pull air through the sampling pipe and the pumps for the membrane filter and the cascade impactor were all started before welding starts. After about 10 seconds of welding, the valves in the connections for the impactor are switched from clean air to welding aerosol collection, which continues for 20-40 seconds. The valves are then switched back and all the aerosol still inside the cascade impactor is allowed to be collected at nominal flow rates before the pump is turned off. About 20 seconds after finishing the welding, the fan and pump were turned off and the filters and impactor plates exchanged in a laboratory completely sealed-off from the welding hall.

RESULTS AND DISCUSSION

TOTAL FUME EMISSION

To facilitate comparison of fume production from different welding techniques, it is convenient to define two entities, viz. the total fume emission rate, E, the total mass of emitted fume in g/min, and the relative fume formation index, R, the total mass of emitted fume normalized to the mass of deposited consumable (excluding slag) in mg fume per g deposited consumable. In Table 2, the total masses of aerosols produced in the different welding processes, expressed in terms of E and R, are summarized. The results selected are for "normal" values of welding parameters and dimensions.

Electrode	Diam.(mm)	I (A)[1]	U(V)[1]	E(g/min)	R(mg/g)
OK 38.65	3.25	160	35	0.58	16.7[3]
OK 38.85	5	300	34	1.30	15.7
OK 38.95	4	210	32	0.93	21.7
OK 38.95[2]	4	205[2]	30[2]	0.75	19.2
OK 48.00	3.25	140	23	0.45	26.0
OK 61.41	3.25	115	33	0.38[3]	11.3[3]
OK 63.35	4	140	24	0.39	15.6[3]
OK 69.21	4	140	22	0.29	12.4
OK 12.51 CO_2	1.2	180	30	0.23[4]	5.4[4]
OK 16.32 Ar	1.2	180	26	0.20	3.8
OK 16.32 Ar/CO_2	1.2	180	26	0.29[3]	5.7
OK 18.01 Ar	1.2	180	22	0.49	20.5
OK 18.13 Ar	1.2	160	24	0.91	24.1
Tungsten, thoriated	-	112	12	0.002	-

1) Direct current; reversed polarity (electrode as anode).

2) Alternating current.

3) Standard error of the mean : 5-10%.

4) Standard error of the mean : 10-15%.

Table 2. The welding situations referred to in the text as "normal" welding, implying that the welding currents were chosen to be in the middle of the intervals recommended by the manufacturers and the welding voltage close to the values recommended. E and R denote respectively the fume emission rate and the relative fume formation index. The standard errors of the mean were less than 5% if not given.

The total fume emission rate is very dependent on electrode dimension and electric power and, due to variation in these parameters, E varies in the interval 0.2 to 2 g/min for the methods in the present study (except for GTAW). As can also be seen from Table 2, large variations in R are found between the different methods (3-35 mg/g). The choice of welding method will strongly influence the ratio between fume production and welding production. However, since this choice is guided also by technical demands and availability and since the comparison does not include the chemical composition of the welding aerosol, it is not always possible or even desirable to choose the method of lowest relative fume formation index. From Table 2 can be inferred that the SMAW methods generally give higher values of both E and R than the GMAW methods. One exception, however, is GMAW for aluminium welding with equally high or even higher values than SMAW.

The results in Table 2 can be compared with those of the systematic study in ref.[2]. The methods in this study with a corresponding or very similar method as in ref.2 are OK 48.00, OK 61.41, OK 63.35, OK 12.51, OK 16.32 and OK 18.13. Both E and R for these methods are in good agreement with the results in ref.2, the differences being normally smaller than 10%. The discrepancies might be explained by somewhat different welding conditions and variations between different brands of welding consumables of the same classification.

SMAW

In Table 2 are given emission results for "standard" welding situations recommended by the the manufacturer. However, when the welding current is raised within the intervals recommended, there will be a significant increase of E reflecting the enhanced melting rate of the consumable. This current dependence seems similar for all SMAW-methods and in fig 5 the fume emission rate is plotted versus welding current (at normal welding voltage). All the methods, dimensions and currents studied are included and it seems that E might be expressed mathematically as $E=a \cdot I^b$. Regression analysis of this power curve gives $a=2.1 \cdot 10^{-4}$ and $b=1.54$ with $r^2=0.88$, indicating a strong dependence of E on current. Since all the data points in fig 5 lie close to the regression line, the seven SMAW-methods in this study, despite their different dimensions, coatings and core compositions, seem to follow approximately the same current dependence when they are used according to the manufacturer's recommendations. These results agree well with those of refs.[2] and 21.

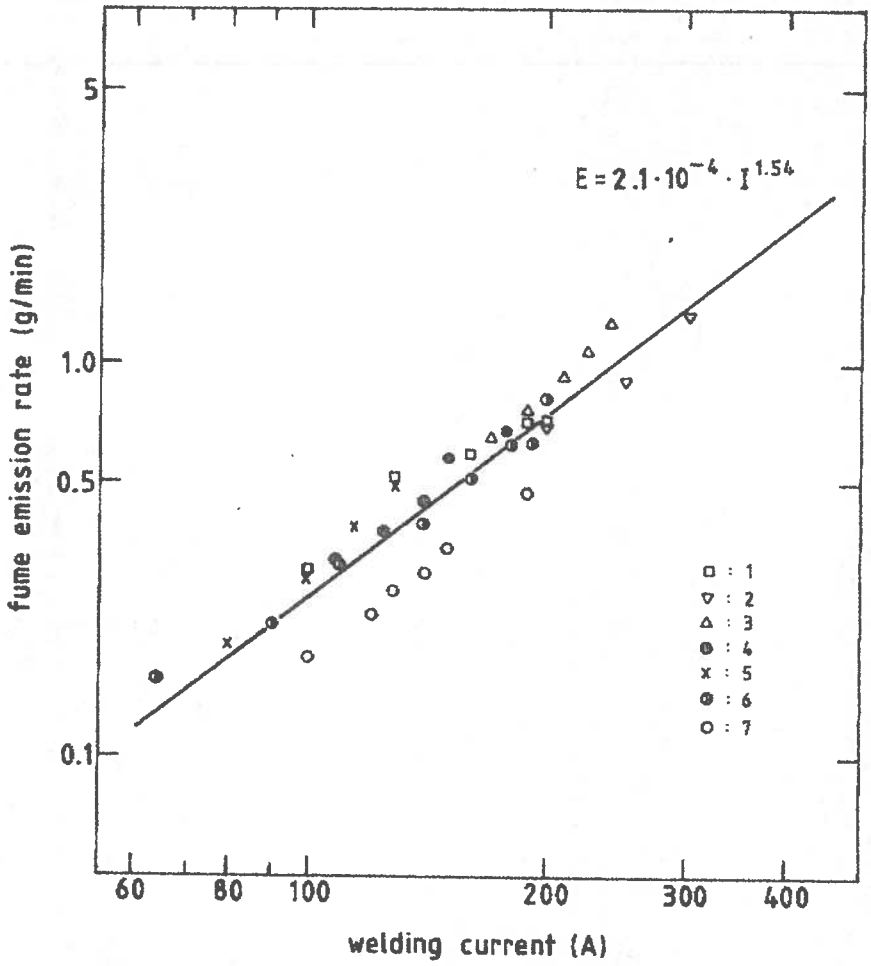

Figure 5. Fume emission rates for all the SMAW-methods in this study plotted versus welding current (r^2=0.88). The number at each symbol refers to the corresponding welding method in Table 1.

For the relative fume formation index R, the influence of welding current is, within the stated current interval, normally rather low, since the increased fume emission rate is mainly the result of an increased melting rate. For some methods, a slight increase in R with current is found, probably because of the increased temperature at the melting tip of the electrode.

In fig 6 and 7 the fume emission rate and the relative fume formation index of three different SMAW methods (for stainless steel) are plotted versus welding voltage. Increases in both E and R are observed with increasing voltage. At high voltage the long electric arc creates increased turbulence and hence facilitates penetration of oxygen through the protective atmosphere formed by the evaporating electrode coating. This oxygen can react with the melted and vapourized metals forming oxides which will promote fume emission since they often have higher vapour pressure than the pure metals. From fig 7, it is evident that the influence of welding voltage on R is dependent of the type of

coating on the electrode in question. Different relations between voltage and arc length are the probable explanation for this. The crater formed by the coating during steady state welding hides part of the electric arc and hence it is very difficult to measure the arc length for direct correlation with R. Since the use of a longer arc causes increased disturbance due to metal spatter and turbulence it also produces a deteriorated welding joint. Hence, keeping the arc length short and welding voltage low, e.g. by keeping the angle between the electrode and the work piece close to 90° [21], should be recommended.

The SMAW methods in this study have normally been welded with DC and reversed polarity. For one method, however, AC is also recommended and in Table 2 E and R are given for this method for both modes of current. The values of E and R are somewhat lower in the case of alternating current but the differences (<10%) are insignificant from the hygienic point of view.

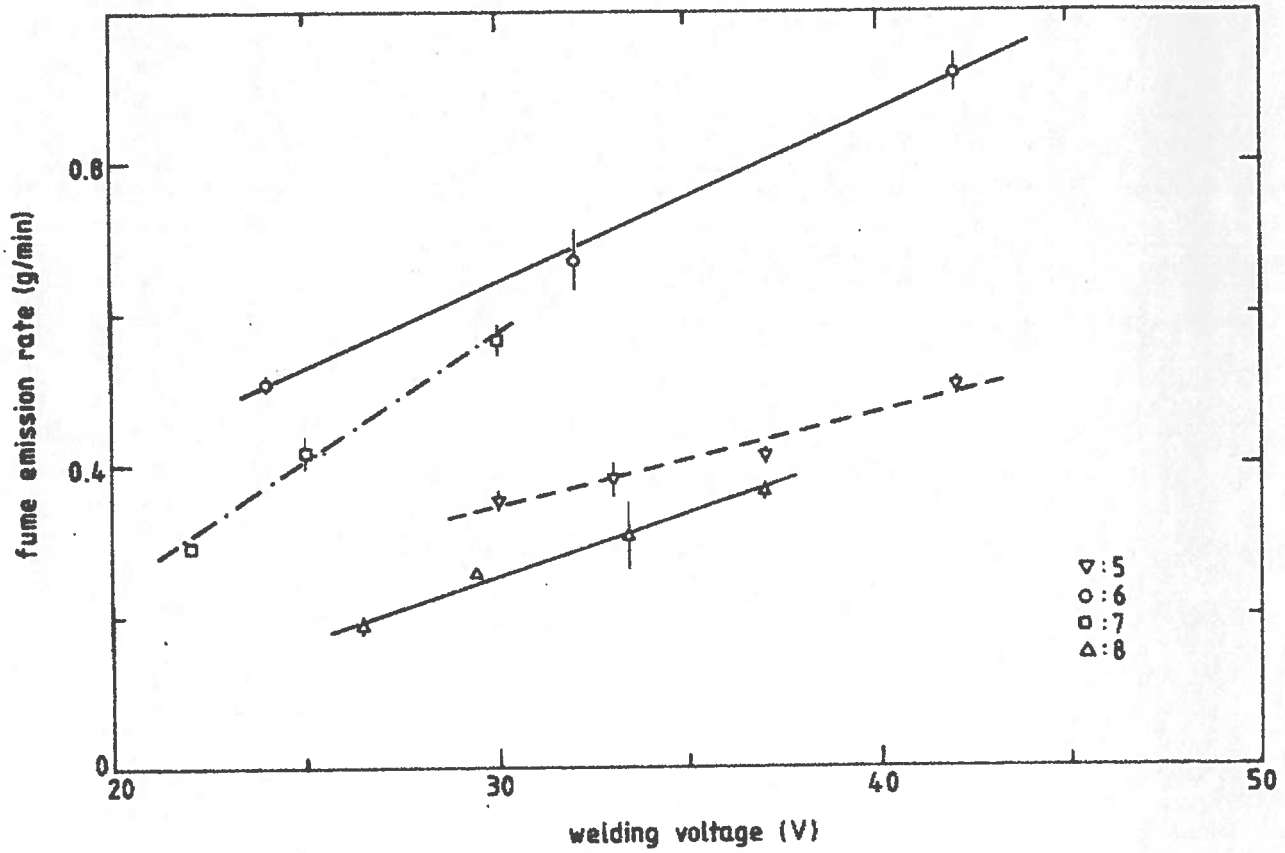

Figure 6. Fume emission rates for three SMAW-methods (stainless steel welding) and for the GMAW method with CO_2 as protective gas (mild steel welding) plotted versus welding voltage. The number at each symbol refers to the corresponding welding method in Table 1. The welding currents were 115, 160 and 140 A for methods 5, 6 and 7 respectively, and 200 A for method 8. The error bars show one standard error of the mean.

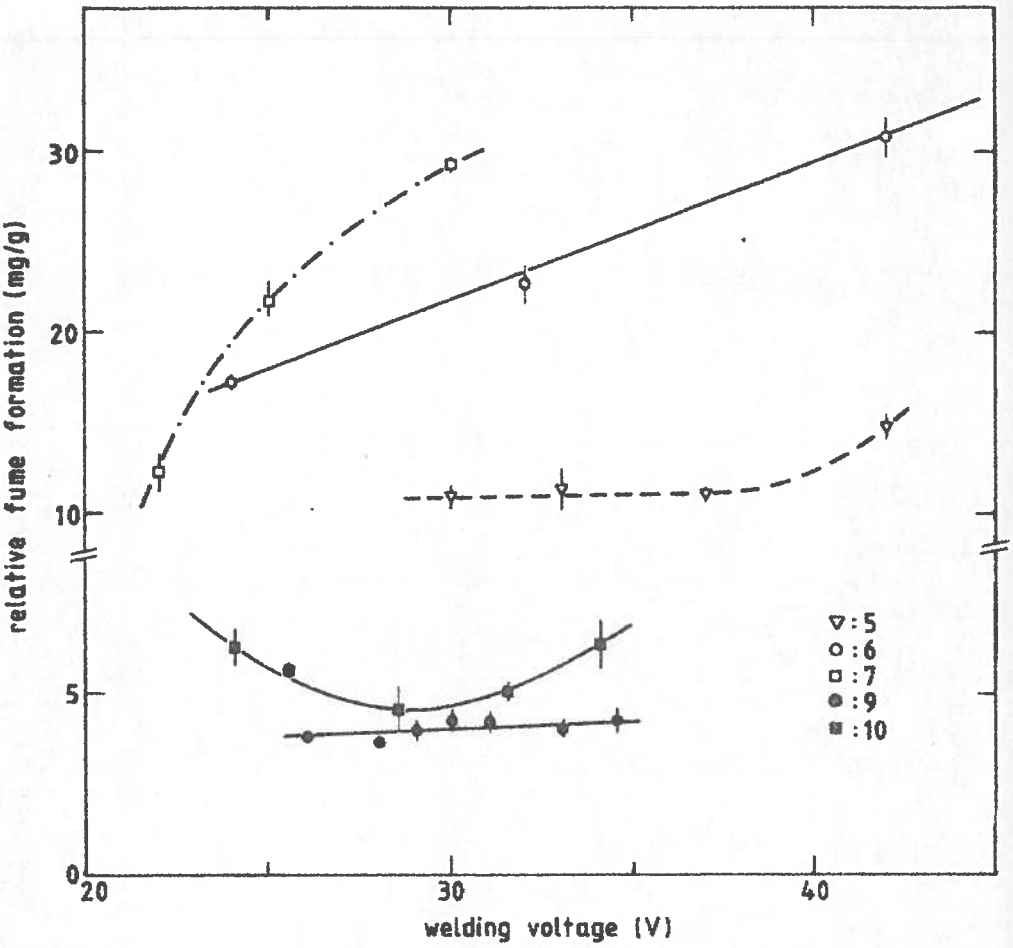

Figure 7. Relative fume formation index plotted versus welding voltage for the same SMAW methods as in fig. 6 and for the GMAW method with pure Ar (●) and Ar/CO_2 (■) as protective gases respectively. The number at each symbol refers to the corresponding method in Table 1. The welding current in method 10 was 180 A. The error bars show one standard error of the mean. Note the shift of scale on the ordinate axis.

GMAW

Semi-automatic methods for gas metal arc welding may appear to be well-controlled and simple physical systems composed of the melting metal wire and the surrounding protective gas. However, due to the influence of the protective gas on the electric arc and on the metal transport process, the fume emission will be a complex function of the welding parameters.

When pure CO_2 is used as a protective gas, the transfer of the melted metal from the electrode tip to the work piece can be characterized as large globules (diameter: 2 to 3 mm) transported by gravity and magnetic forces. The sizes of the globules are virtually unchanged when the welding parameters are altered. If, however, the protective gas is argon or mixtures of argon and CO_2 , two different modes of transfer will be possible. With low voltage and low current the transfer will be globular with decreasing sizes and increasing numbers of

globules for increasing current. For high voltage, at a certain critical value of current, the transition current, a very abrupt change in the size and frequency of the globules takes place and metal transfer becomes a spray of very small droplets (diameter: 0.5–1 mm). The drop size remains rather constant when the current is increased and instead the number of droplets per unit time increases. The detachment of the small droplets from the electrode is due partly to the magnetic "pinch effect" and transport along the arc is due mainly to the plasma jet[22] . The value of current at which this transition occurs is proportional to the diameter of the electrode and dependent on the material and electrode extension[23] .

When mixtures of argon are used, the gas with which it is mixed changes the properties of the protective atmosphere and hence the fume formation process will be altered. In fig 7 the relative fume formation index is plotted versus welding voltage with pure argon and with a mixture of 80% argon and 20% CO_2 as protective gases, respectively. While, for pure argon, R is rather independent of the welding voltage, there is a well-defined minimum at a specific voltage for the Ar/CO_2 case. The magnitude of R is also higher for all voltages when CO_2 is mixed into the gas and hence the oxidizing potential of the atmosphere surrounding the arc is increased. The oxides of several elements have higher vapour pressure than the pure elements, thus promoting fume formation in a oxidizing atmosphere. This effect has been shown in detail in refs. 3 and 24.

The welding current for OK 16.32 in fig 7 (I=180±5 A) is above the transition level for this particular electrode with a diameter of 1.2 mm [25]. To establish a stable spray arc, the voltage (arc length) has to exceed a certain value, which in the case of pure argon was about 30 V and for the Ar/CO_2 mixture 28 V. The minimum in R in fig 7 for the Ar/CO_2 mixture coincides with the lowest voltage at which a stable spray arc can exist. Once a stable spray arc is established, R will increase with voltage in case of Ar/CO_2 gas but remain constant for pure Ar. The increased voltage corresponds to a longer electric arc with a consequently longer residence time for the droplets in the oxidizing atmosphere while being transferred to the work piece, and hence, according to what is stated above, an incresed probability for fume formation. The inert Ar-atmosphere which surrounds the arc protects the droplets from oxygen during transfer and essentially all fume will be produced, mainly due to vaporization, close to the melting tip where the temperature is very high.

In pure CO_2-welding the fume emission rate increases strongly with voltage, as can be seen from fig 6. This dependence is in good agreement with the results of refs. 26 and 27, where the same or very similar welding parameters have been used. If, instead, the welding current is increased at constant voltage, the wire feeding speed increases with a decreasing length of the welding arc[26]. In fig 8 the relative fume formation index versus current is plotted for constant voltage. Due to the decreasing transition time for the globules in the CO_2 -atmosphere, R decreases with increasing current (compare ref.3).

It is evident from the findings above that gas metal arc welding constitutes a complex field as far as the emission of welding fumes is concerned and that all welding parameters and conditions have to be stated precisely for adequate comparison of research results and finally that the choice of shielding gas has a significant influence on the fume emission characteristics.

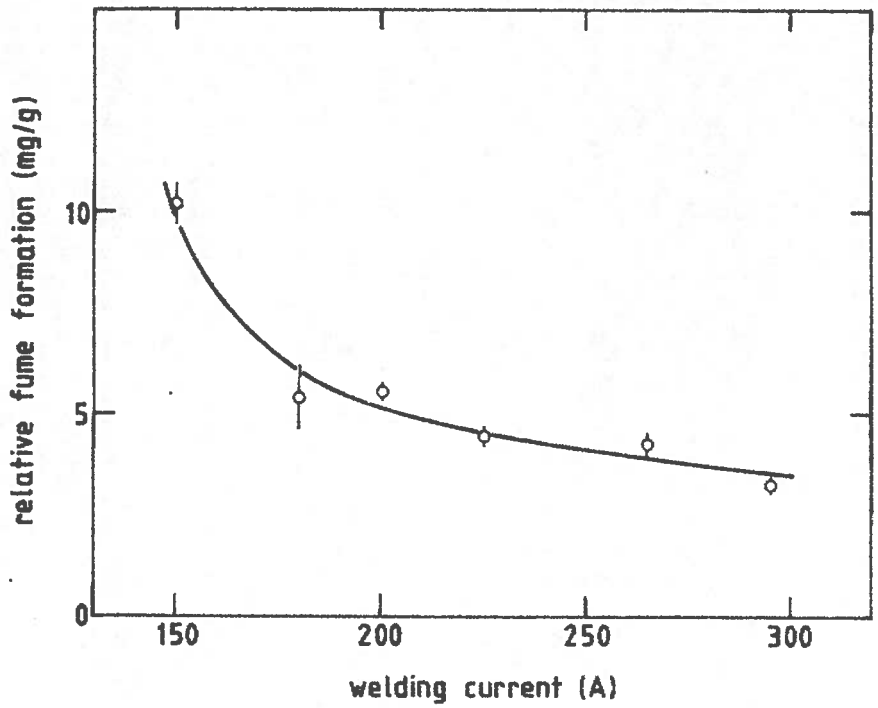

Figure 8. Relative fume formation index plotted versus welding current (U=30 V) for GMAW welding of mild steel with CO_2 as protective gas. The error bars show one standard error of the mean.

ELEMENTAL COMPOSITION

In Table 3, the elemental composition of welding aerosols from the different welding processes are given for the same parameter values as those in Table 2. The part of the aerosol which has not been analysed contains such elements as oxygen, nitrogen, sodium and silicon.

	Elements														
No.[1]	F	Cl	K	Ca	Ti	Cr	Mn	Fe	Ni	Cu	Zn	As	Rb	Zr	Mo	Pb
1	7.1		8.8	2.6		.07	5.9	32		.08	.17[3]	.06[3]		.54		.10[3]
2	11	.26[3]	15	.62	.54		4.7	24			.29[4]					
3	11	.33[3]	15	2.0			3.4	23			.04[3]			.23[3]		.07[3]
3[2]	14	.54[3]	19	1.8			2.8	11			.04[3]			.36[3]		.07
4	16		16	9.5	.45	.04	3.7	19		.01	.13	.03[3]				
5	21		18	1.3	2.1	3.4	2.4	3.7	.22	.01	.25		.02			
6	24	.34	22	10	.62	3.1	2.7	3.3	.24		.11		.01		.03	.03
7	16	.20	22	3.5	2.3	3.0	14	3.4	.44[3]		.14				.09[3]	.04[3]
8						.07[4]	7.3	45		.26[3]	.04[4]					
9						10	5.3	28	4.5	.06	.17				.95	
10						12	4.8	31	4.8	.09	.18				.92	
11						.02[4]		.12[4]		.03						
12						.04	.14	.06			.02					

1) See Table 1; 2) Alternating current; 3) Standard error of the mean : 10-20%
4) Standard error of the mean : >20%

Table 3 . Relative elemental compositions (expressed as a per cent of the total mass of aerosol) of the welding fumes from the welding situations described in Table 2 as determined by PIXE analysis. The standard errors of the mean are less than 10% if not explicitly shown. Due to its low total emission GTAW is not included.

Basically, the elemental composition of a welding aerosol reflects the composition of the consumable electrode used insofar that the elements present in the welding consumable are also found in the aerosols but normally with their relative abundances altered. In the electric arc column the highest temperature is found at the axis near the melting tip of the electrode[28] . Consequently, metal vapours will come mainly from the welding electrode and from the surface of the metal droplets being transferred in the arc. This statement is supported by the findings in ref. [29] in which a systematic study was carried out to

determine the site of aerosol production in SMAW-methods. Known concentrations of chromium, manganese and nickel were added to coating, core wire and workpiece respectively. By elemental analysis of the welding aerosol the contributions from the different sites were estimated, and the core wire was found to be the dominating source of these metals in the aerosol. One consequence of this finding is that the choice of work piece composition is not very critical in welding aerosol studies. It is, however, very important to check that no surface contaminations, such as metal primers, are present since they may be much more volatile and will contribute significantly although they emanate from the low temperature zone of the arc.

In Table 4 are given fractionation factors of the different metals in the welding aerosol relative to the welding consumable for four different welding methods. Noticeable are the high factors for manganese (2-7) while the factors of the other elements are well below unity. This is in good agreement with the results from the above study[29] . Since manganese has a much higher vapour pressure than, e.g. chromium and nickel, it will also have a higher tendency to fume formation and occur in relatively higher concentrations in the welding fumes as compared to the work piece.

	Shielded metal arc welding		Gas metal arc welding	
	Low alloy electrodes (n=4)	Stainless steel electrodes (n=3)	CO_2 - gas Low alloy steel (n=1)	Argon - gas Stainless steel (n=2)
Cr		0.17-0.21		0.68-0.70
Mn	2.2-6.1	2.3-3.8	6.9	4.2-5.2
Fe	0.22-0.33	0.055-0.066	0.49	0.47-0.50
Ni		0.025-0.040		0.36-0.41
Mo		0.027-0.052 (n=2)		0.24-0.32

Table 4. The elemental concentrations in the fumes divided by the elemental concentrations in the welding consumables. The intervals are defined by the minimal and maximal values. n = the number of methods included.

SMAW

The welding parameters, mainly the voltage, affect the elemental composition of the welding aerosol. In fig.9 are plotted the relative abundances of five different elements in the fume from a stainless SMAW-method versus welding voltage, showing increasing concentrations for the three core wire metals chromium, manganese and iron and decreasing concentrations of fluorine and potassium which originate from the electrode coating. For other electrodes, the voltage dependence is not exactly the same, but nevertheless the same groups of

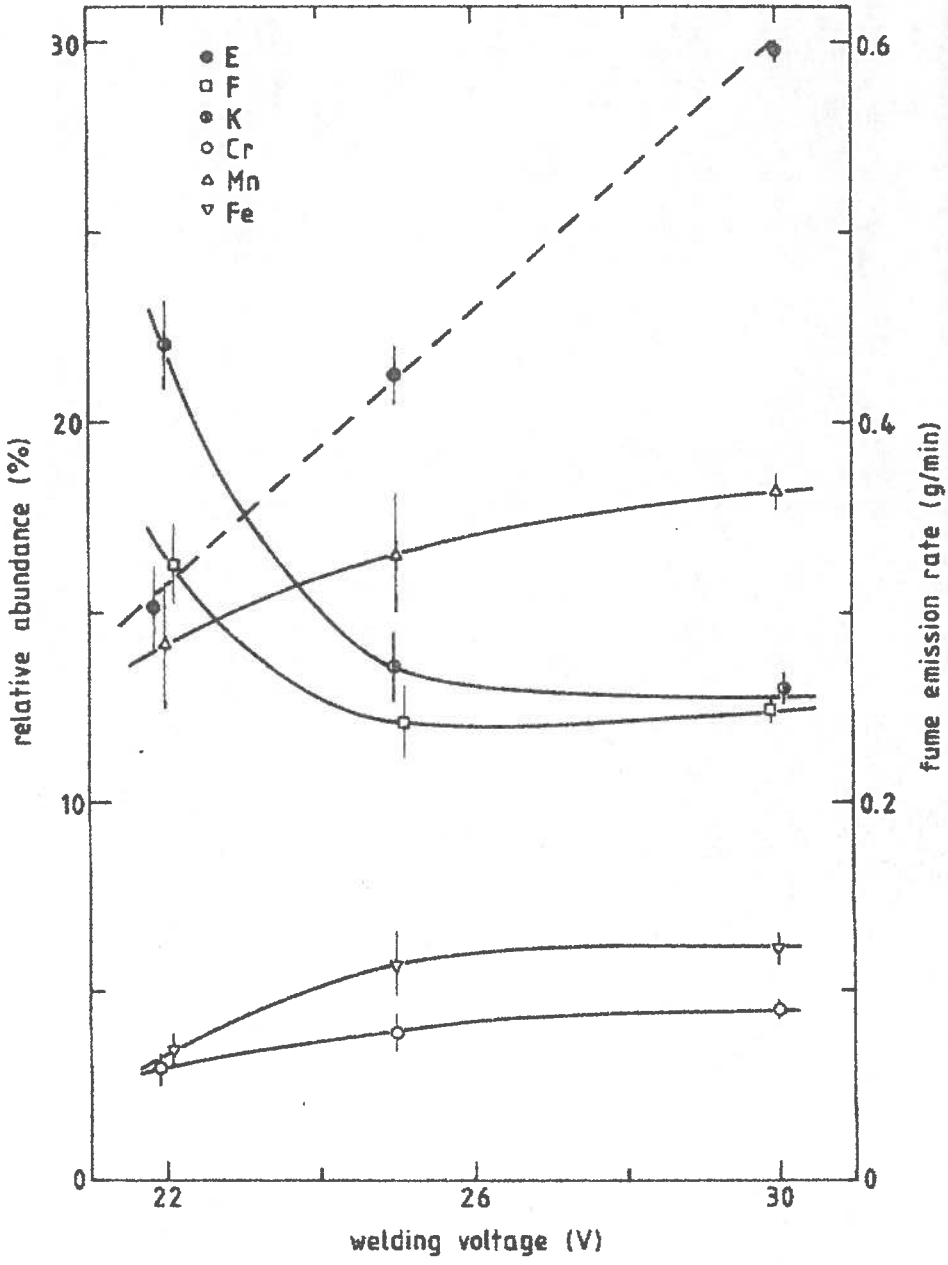

Figure 9. Relative elemental abundances (left-hand axis) in the fumes from welding stainless steel with a SMAW-method (OK 69.21, diam.:4 mm and I=140 A) plotted versus welding voltage. To facilitate estimating the absolute elemental emission, E is also plotted (right-hand axis). The error bars show one standard error of the mean.

elements develop, e.g. potassium and fluorine represent one category of elements following similar patterns of variation and chromium, manganese, iron and nickel normally another. The reasons for these variations may be the resemblance in chemical and physical properties and/or in the distribution of the elements in the electrode. The distinct voltage dependence of the elemental composition is probably explained by the variation in arc length. In fig.9 the dependence of the fume emission rate on voltage is also included in order to show how the absolute emissions of these elements vary with voltage.

Welding is normally performed in the DC mode and with reversed polarity but in some methods AC is also used. For one of the methods studied here, the change to AC causes a drastic change in the relative composition (compare Table 3). The temperature at the electrode tip depends on the polarity and consequently the use of an alternating current is expected to change the conditions for fume production and hence the chemical composition.

GMAW

In the semi-automatic GMAW-methods no protective electrode shielding is used and the composition of the welding fumes is determined by the composition of the metal wire and by the protective gas.

Gas metal arc welding of mild steel is normally performed in a 100% CO_2 atmosphere giving globular transfer as described above. When the welding parameters are varied, no significant variation in the elemental composition has been observed in the present study. This and the relative abundances of Mn and Fe observed are in good agreement with the results from other studies of the same process [3,30].

It was shown above that a protective atmosphere of argon affects the fume emission characteristics since metal transfer varies with welding parameters. In fig 10, it is shown that the same effect is found in the elemental composition. The relative abundances of two elements in the fume during the welding of stainless steel are plotted versus welding voltage (100% Ar = o, Ar/CO_2 = □). To allow estimates of the absolute mass emissions of the elements, the fume emission rate is also plotted. All metals except manganese have higher relative abundance with Ar/CO_2 than with pure Ar. For both protective gases, the general trend for both elements is to increase with voltage. However, in pure Ar gas, a

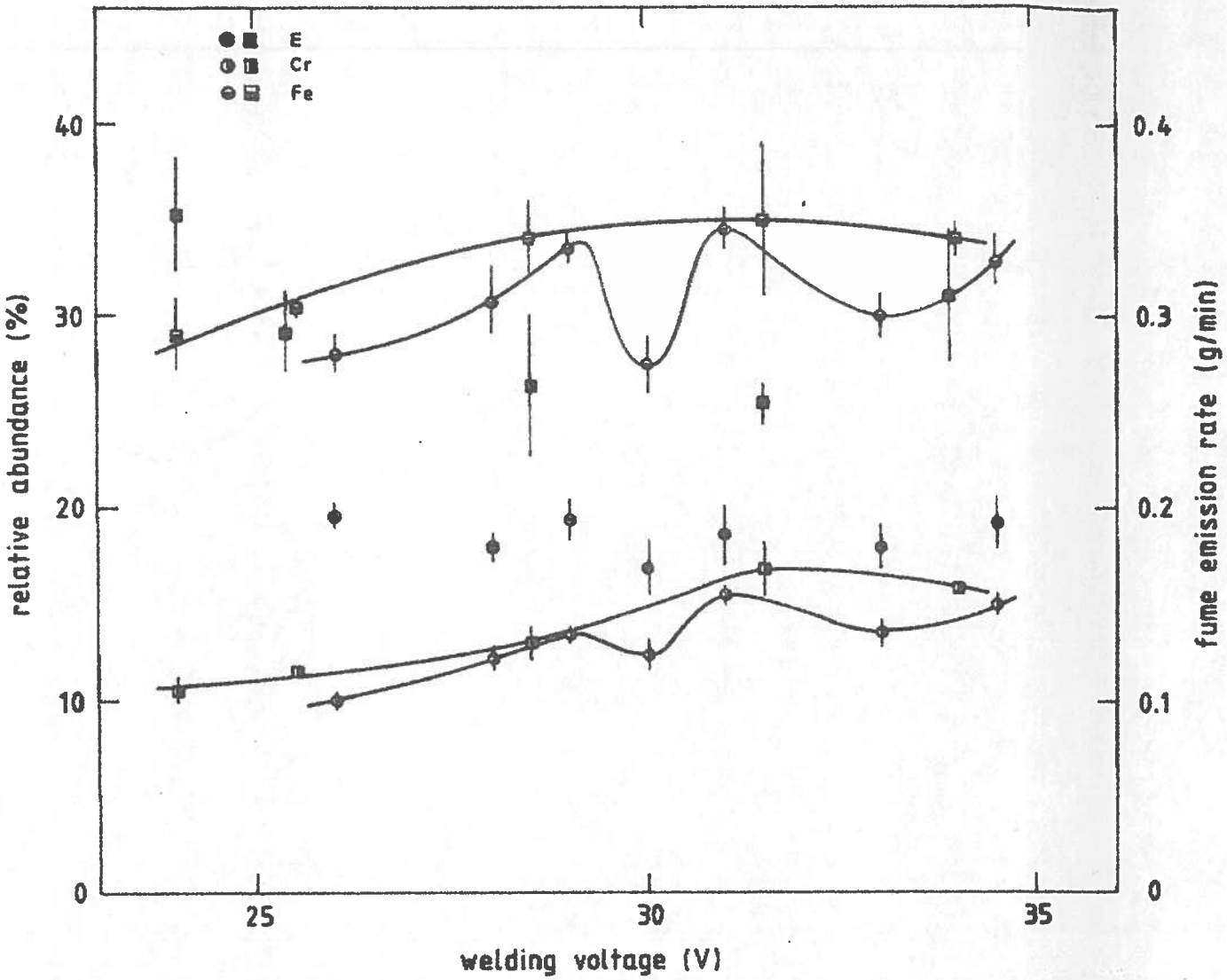

Figure 10. Relative elemental abundances (left-hand axis) in welding stainless steel with GMAW (OK 16.32, I=180 A) and 100% Ar (o) and Ar/CO_2 (□) as protective gases, respectively, plotted versus welding voltage. To facilitate estimating the absolute elemental emission, E is also plotted (right-hand axis). The error bars show one standard error of the mean.

fine structure with dips in the relative abundance at the lowest voltage (approx. 30 V) at which a stable spray transfer can exist is noticed. A similar dip is not observed at the corresponding voltage (approx. 28 V) in the case of Ar/CO_2. A tentative explanation for this fine structure and the difference between the gases is the establishment of a very stable arc essentially free from spatter and turbulence at a critical voltage, assuming the current is high enough, i.e. above the transition current. When pure Ar is used, the oxidizing agents come primarily from the surrounding air and their penetration is significantly reduced because of the very stable arc. With 20% CO_2 in the gas, the oxygen in CO_2 will be the dominant oxidizing agent and the influence of the surrounding air is less pronounced.

GTAW

Since the total fume emission is very low for GTAW and pure Ar as the protective gas, no results on the elemental composition of the aerosols formed are included in Table 3. However, apart from Fe, Mn, Cr, Ni, Cu and Zn, traces of W are also found.

OXIDATION STATE OF CHROMIUM

An analytical routine developed for determinations of chromium oxidation state[15] was applied to stainless steel welding aerosols from three SMAW-methods and one GMAW-method. The results are shown in Table 5. For GTAW of stainless steel, the total fume emission was too low for this analytical procedure to be used. In aerosols from the three SMAW-methods for stainless steel welding, more than 50% of the chromium is soluble and hexavalent. Between 60 and 100 % of the chromium in the particle surface layers is hexavalent as determined by ESCA-analysis, but decreases after washing the aerosol with a buffer solution (pH 7.4). Apparently most of the hexavalent chromium on the particle surfaces leaches out during washing. The formation of hexavalent chromium is dependent on which elements have been added to the coating and it has been shown by Kimura et al[31] that it is possible to reduce the amounts of hexavalent chromium by changing the additives to the coatings and still perform technically adequate welding.

Method number[1]	Diam. (mm)	I(A)	U(V)	Cr-tot (%)	A	B	C
5	3.25	100	35	3.4	.50	.60	.27
6	3.25	100	22	4.4	.73	1.00	<.15
7	3.25	105	21	2.9	.52	1.00	<.15
9	1.2	180	26	12	.019	<.15	<.15

1)= see table 1

A = Cr(IV)-soluble/ Cr-total.

B = Cr(VI)/Cr-total on the particle surfaces.

C = Cr(VI)/Cr-total on the particle surfaces after washing.

Table 5. Results from determinations of oxidation state and solubility of chromium in welding aerosols from stainless steel welding.

Transmission electron microscopy (TEM) gives information on the structure of individual welding particles for interpreting the ESCA-results. The aerosol particles from the SMAW methods appear as chains or agglomerates of smaller particles (<0.1 µm in geometric diameter). The chains are surrounded by shells with lower electron density than the particles in the core. The ESCA analysis of unwashed particles is just valid for the outer layer of these shells. After washing, a large fraction of the shell has been dissolved and information on the core material is obtained from ESCA. The TEM studies have shown that after washing, the core particles consist of smaller homogeneous particles with diameters of about 0.01 µm. The ESCA results are representative of about 80% of the volume of particles of this size.

The washing procedure separates the readily soluble Cr from less soluble, in a well-defined way. However, from the toxicological point of view, the separation of these fractions is not well-defined, because of the uncertainty of the hygienic significance of differences in the solubilities of various chromium compounds. In a particle of welding aerosol, the chromium is present in a complex environment and the solubility found in the washing procedure may not, in a simple way, be relevent to the solubility of a given chromium compound in the airways.

Chromium oxidation state results for argon gas metal arc welding are quite different from SMAW-results. Only about 2% of the total chromium is soluble and hexavalent and for both the unwashed and washed aerosol samples the concentrations of hexavalent chromium on the particle surfaces are below the detection limit of the ESCA method (<15%).

The results indicate that, although the aerosols from them have lower relative abundances of total chromium, the use of SMAW-methods would imply significantly higher health hazards than the use of GMAW-methods. Switching to the latter methods, however, may not always be possible for technical reasons. Further, when comparing the health hazards of these two classes of welding, other aspects, such as the hazardous gases emitted during welding have to be taken into consideration. In most processes NO_x is formed and in GMAW and GTAW also considerable amounts of the strong irritant ozone (O_3). Discussions or measurements of these gases have been beyond the scope of this study and hence the conclusions about possible health effects of the SMAW, GMAW and GTAW processes reached here do not include the influence of hazardous gases formed during welding.

Within the uncertainties of the differences in welding conditions and parameters, the results about the content and oxidation state of chromium in welding aerosols found here are consistent with those of other studies[32-34].

PARTICLE SIZE DISTRIBUTION

In Table 6 the mass median aerodynamic diameters (MMAD), as determined by the Battelle cascade impactor, are summarized. A typical value of the geometrical standard deviation of the distributions is 1.5. The MMAD-values are calculated from PIXE-analysis of the impactor stages and expressed as the MMAD for each element separately. In the case of gas tungsten arc welding the particles are so small that about 75% of the detected mass is found on the after-filter of the impactor and the MMAD value is thus less than 0.25 µm which is the 50% cut-off diameter of the last impaction stage. The mass median aerodynamic diameters for the other methods vary from 0.3 µm to about 0.6 µm. Hence the particles are respirable and have a high probability of deposition in the lower parts of the

	Mass median aerodynamic diameter (µm)								
Electrode	F	Al	K	Ca	Ti	Cr	Mn	Fe	Ni
OK 38.65	.34		.32	.36			.33	.33	
OK 38.85			.45				.45	.45	
OK 38.95			.48				.48	.48	
OK 48.00	.48		.50	.44	.50		.46	.44	
OK 61.41			.39	.43	.39	.38	.39	.39	.35
OK 63.35			.39	.39		.39	.39	.42	
OK 69.21						.47	.49	.30	
OK 12.51[1]							.32	.33	
OK 16.32[2]						.31	.30		.32
OK 16.32[3]						.34	.34	.35	.34
OK 18.01[2]		.42							
OK 18.13[2]		.37							

1) 100% CO_2; 2) 100% Ar; 3) 80% Ar and 20% CO_2

Table 6. Mass median aerodynamic diameter for different elements and welding methods as determined by the Battelle cascade impactor and PIXE analysis.

respiratory tract. In other welding aerosol studies, only a few particle size distribution determinations have been reported. The results of refs. 2,3,4,5,9,27 are essentially in agreement with those of the present study. The low MMAD values found in GTAW indicate that the high arc temperatures in this type of welding (approx. 10000 K) together with the basically non-melting electrode, made from thoriated tungsten, promote the formation of very small particles.

The particles emitted in SMAW-methods contain significant concentrations of highly soluble and hygroscopic compounds derived from elements such as F, K and Na in the electrode coating. The high relative humidity of the human respiratory tract, RH >99% in the subglottic region[35], makes the particles rapidly absorb water, which may significantly alter the patterns of deposition there.

Particle size determinations have been carried out for all methods and sets of parameters. When the welding parameters are changed, only negligible variations (<10%) of the particle diameter will occur. The variation of the MMAD between elements for a certain method is also negligible. The particle formation process normally includes evaporation, oxidation and condensation steps[3]. The process has been shown to be sensitive to the welding parameters in producing different compositions and mass concentrations but apparently this is not reflected in the particle sizes, but rather in the number concentration of the aerosols. One important implication of these results is the possibilty of using a simplified method to characterize welding aerosols including only a few particle size determinations for each method. The particle size determination is rather tedious and complicated insofar as sampling and analysis are concerned and a reduction in the number of determinations will save substantial time and effort.

SUMMARY

Several welding methods were characterized using a specially designed collection apparatus which has been found to be reliable and to yield accurate and representative sampling of welding aerosols. Special requirements of very low air velocity around the welding place and the possibility of testing the GMAW methods in automatic mode excluded the use of the standardized "Swedish fume box"[36]. The analytical facility of Particle Induced X-ray Emission was a prerequisite for this extensive and detailed study. The PIXE method, with complementary nuclear methods, is very well suited to the study of work environment aerosols in general[14] and welding aerosols in particular, in that it yields complete quantitative information of many important elements at a low cost. Furthermore, as compared to traditional techniques it significantly simplifies particle size determination.

The highest fume emission in this study is found for SMAW methods followed by GMAW of aluminium and GMAW of steel. By far the lowest emission is found for GTAW of stainless steel. The fume emission rate (E) is determined primarily by the welding current and a similar current dependence is found for all SMAW methods if welded at normal voltage. The voltage also affects E but to a smaller extent. The relative fume formation index (R) varies drastically among the methods and is dependent on the welding parameters. For gas metal arc welding of mild steel with pure CO_2 as the protective gas, R decreases with increasing current.

The composition of the shielding gas in GMAW is important for the fume production. R is higher in the case of the Ar/CO_2 mixture than in the case of pure Ar. The influence of the welding parameters on fume formation is altered by mixing CO_2 into Ar. This study supports the findings of earlier works, viz. that the oxidizing potential of the gas surrounding the electric arc is of considerable importance in determining the fume production, with increased fume production when increasing the oxidation potential of the protective gas.

The elemental composition of a welding aerosol is dependent on the method but also on the welding parameters, primarily the voltage. The fume contains the same elements as does the consumable but with the relative abundances changed due to fractionation effects during aerosol formation. This is explained by the different properties of the elements, e.g. with regard to vapour pressures of the pure elements and their compounds. For SMAW with the recommended voltage,

only minor variations occur when the current is changed. Welding voltage and current mode (AC/DC) have drastic impacts on the elemental composition of the fumes. This is probably due to changes in electric arc length and arc characteristics respectively. The elemental composition of a GMAW aerosol is also dependent on the protective gas. Thus, a relative decrease in several elements is noted when the transition from globular to spray transfer takes place in an Ar atmosphere. The complexity of fume formation processes and the growing popularity of GMAW methods in industry due to increased production and welding quality stresses the need for further studies within this field.

The fumes produced from SMAW and GMAW methods when welding stainless steel clearly show the great differences between these two main types of welding procedures. While the chromium in the SMAW aerosols is almost entirely hexavalent (and soluble), only trivalent chromium is found in the GMAW aerosols. The well-known difference in biological activity between the two oxidation states of Cr is reason enough to infer that, if possible, GMAW methods should be chosen when welding stainless steel.

The particles in the welding aerosols are below 1 μm in diameter and consequently respirable and able to reach the lower parts of the human respiratory system. Mass median aerodynamic diameters vary from well below 0.25 μm to 0.6 μm and seem to be rather independent of the welding parameters. An important factor in evaluating the deposition of aerosols from SMAW methods is the hygroscopicity of the particles which, in the high humidity of human airways, may cause changes in the aerodynamic properties of the particles.

ACKNOWLEDGEMENTS

We are indebted to Dr F. Brundin for many stimulating discussions throughout this work and for putting welding equipments and other resources at our disposal. The skilled and patient welding of hundreds of welding joints by Mr. Alex Simonsson is gratefully acknowledged as is much good advice throughout the course of this study.

We have highly appreciated the equipment built by Mr Knut Sjöberg throughout this investigation.

This investigation has been supported financially by the Swedish Work Environment Fund.

REFERENCES

1. J. Moreton and N.A.R. Falla, Analytical Sciences Monographs No 7, The Chemical Society, London (1980).

2. Fumes and Gases in the Welding Environment, American Welding Society, Miami (1979).

3. R.F. Heile and D.C. Hill, Weld. Journal, 54, 7 (1975) 201-s.

4. The Welding Environment, American Welding Society, Miami (1973).

5. R.M. Stern, "The production and characterization of a reference standard welding fume", Part 2, SVC/SF 78-08, The Danish Welding Institute, Copenhagen (1978).

6. K.G. Malmqvist, G.I. Johansson, M. Bohgard and K.R. Akselsson, "Welding air pollution — characterization of welding fumes", Tables of results translated from Swedish, LUTFD2/TFKF-3025, Lund Institute of Technology, Lund (1980).

7. B.Y.H. Liu and G.A. Kuhlmey, in X-Ray Fluorescence Analysis of Environmental Samples, Ed. T.G. Dzubay, Ann Arbor Science, Ann Arbor (1977) 107.

8. C.N. Davies, Brit. J. Appl. Phys.,Ser.2, 1 (1968) 921.

9. I.M. Naumenko and L.V. Ferdman, Svar. Proizvod. 8 (1974) 50, in Russian.

10. R.I. Mitchell and J.M. Pilcher, Ind. and Eng. Chem., 15 (1959) 1039.

11. P. Gormley and M. Kennedy, Proc. Roy. Irish Acad., 52 A (1949) 163.

12. K.G. Malmqvist et al, to be published.

13. S.A.E. Johansson and T.B. Johansson, Nucl. Instr. and Meth. 137 (1976) 473.

14. M. Bohgard, K.G. Malmqvist, G.I. Johansson and K.R. Akselsson, Nucl. Instr. and Meth., 181 (1981) 459.

15. M. Bohgard, B.L. Jangida and K.R. Akselsson, Ann. Occup. Hyg., 22 (1979) 241.

16. K.G. Malmqvist, G.I. Johansson and K.R. Akselsson, to be published.

17. NIOSH-Criteria Document for Chromium VI, U.S. Dept. of Health, Education and Welfare, Publ. No. 76-129 (1975).

18. K. Siegbahn, C. Nordling, A. Fahlman, R. Nordberg, K. Hamrin, J. Hedman, G. Johansson, T. Bergmark, S.-E. Karlsson, I. Lindgren and B. Lindberg, Atomic, Molecular and Solid State Structure Studied by Means of Electron Spectroscopy, Almqvist & Wiksell (1967).

19. E.B. Sandell, Colorimetric Determination of Traces of Metals, Interscience Publishers, 3rd Ed. (1959) 392.

20. T.A. Cahill, Aerosol Measurement , Ed. D.A. Lundgren, University Presses of Florida, Gainesville (1979) 131.

21. M. Kobayashi, S. Maki and J. Ohe, Int. Inst. of Welding, Doc VIII-670-76, (1976).

22. J.C. Needham, C.J. Cooksey and D.R. Milner, Brit. Weld. J., 7 (1960) 297.

23. A. Lesnewich, Weld. Journal, Sept (1958) 418-s.

24. I.R. Patskevich and O.A. Rykov, Avt. Svarka, 8 (1971) 15, in Russian.

25. L.F. Defize and P.C. van den Willigen, Brit. Weld. J. 7 (1960) 297.

26. B. Haas and H.V. Pomaska, Proc. of Coll. on Welding and Health (1980) No 10.

27. F. Eichorn and F. Trösken, Industrie Anzeigen, 101 (1979) 31, in German.

28. L.A. King and J.A. Howes, Proc. Physics of the Welding Arc, (1962) 180.

29. M. Kobayashi, S. Maki, Y. Hashimoto and T. Suga, Weld. in the World., 16, No 11/12 (1978) 238.

30. M.J. Erman, E.E. Raiskiy and A.G. Potapevskiy, Autom. Weld., 21, No 4, (1968) 65.

31. S. Kimura, M. Kobayashi, T. Godai and S. Minato, Proc. of Coll. on Welding and Health (1980) No 16.

32. G.M. Lautner, J.C. Carver and R.B. Konzen, Am. Ind. Hyg. Ass. J., 39 (1978) 651.

33. S. Kimura, M. Kobayashi, T. Godai and S. Minato, Weld. Journal, 58 (1979) 195-s.

34. E. Thomsen and R.M. Stern, Scand. J. Work Environ. Health, 5 (1979) 386.

35. J. Postendörfer, J. Aerosol Science, 2 (1971) 73, in German.

36. G. Gerhardsson, Int. Inst. of Welding, Doc. VIII-629-75 (1975).